

## **Renal cortical remodelling by NO-synthesis blockers in rats is prevented by angiotensin-converting enzyme inhibitor and calcium channel blocker**

**C. A. Mandarim-de-Lacerda \*, Leila M. M. Pereira**

*Laboratory of Morphometry & Cardiovascular Morphology, Biomedical Centre,  
Institute of Biology, State University of Rio de Janeiro (UERJ), Brazil*

*Received: July 13, 2001; Accepted: September 3, 2001*

### **Abstract**

The cortical remodelling was studied when chronically nitric oxide synthesis (NOs) blockade (L-NAME-induced) hypertensive rats are simultaneously treated, or not, with angiotensin-converting enzyme inhibitor or calcium channel blocker. Four groups of eight rats each were studied as follows: Control (C), L-NAME (L), L-NAME+Enalapril (L+E) and L-NAME+Verapamil (L+V). The systolic blood pressure (SBP) was weekly recorded. The cortex of the left kidneys was analysed according to the vertical section design. The volume-weighted mean glomerular volume (VWGV) was made through the "point-sampled intercepts" method. Enalapril and verapamil were efficient in reducing the SBP in rats submitted to NOs blockade. Glomeruli had considerable alterations in L group rats (glomerular hypertrophy or sclerosis) and tubular atrophy. The VWGV was 100% greater in L group rats than in the C group rats, while it was 30% smaller in L+E and L+V groups than in L group. The tubular volume was 30-50% greater, while the tubular length was 20-30% smaller in the L group than in the other groups. The renal cortical region showed glomerular sclerosis/hypertrophy and tubular remodelling in rats with NOs blockade that was efficiently prevented with the simultaneous treatment with enalapril or verapamil.

**Keywords:** hypertension • kidney • nitric oxide • renin-angiotensin system • calcium channel blocker • ACE inhibitor • glomerulus • morphometry • stereology

### **Introduction**

The nitric oxide (NO) is a small hydrophobic gas molecule synthesized from L-arginine by a process that can be competitively inhibited by L-arginine analogues, such as L-NAME [1]. The NO synthesis

(NOs) has a major physiological regulator function on vascular resistance and renal hemodynamics, as well as on proximal tubular reabsorption activity [2].

The chronic NOs blockade has a great impact on renal hemodynamics, causing marked vasoconstriction, reduction of glomerular filtration rate, and proteinuria [3-4]. In this case the renal blood flow decreased, approximately 25%, reducing sodium excretion without reductions in filtered load, suppressing the slope of the arterial pressure-mediated response in sodium excretion [5-6]. The

---

\* Mail to: Prof. C. A. MANDARIM-de-LACERDA, MD, PhD, Laboratório de Morfometria & Morfologia Cardiovascular, Centro Biomédico, Instituto de Biologia, Universidade do Estado do Rio de Janeiro (UERJ), Av, 28 de Setembro, 87 (fds), 20551-030 Rio de Janeiro, RJ, Brasil.  
Phone/Fax: [+55.21] 2587.6416  
Email: mandarim@uerj.br ; HomePage : www2.uerj.br/~lmmc

NO plays also a major role in regulating proximal tubular reabsorption of water, sodium, bicarbonate, and phosphate, NO regulates Na<sup>+</sup>-K<sup>+</sup>-ATPase, Na<sup>+</sup>/H<sup>+</sup> exchangers, and paracellular permeability of proximal tubular cells, which may contribute to its effect on proximal tubular transport. The final effect of NO on proximal tubular reabsorption appears to depend on the concentration of NO and involves the interaction with other regulatory mechanisms [7].

The progressive hypertension developed and maintained when NOs is inhibited is Angiotensin II dependent, and produces glomerular-vascular injuries, including glomerular sclerosis and ischemic damage [8-9]. The glomerular hypertrophy has been considered an important step preceding glomerular sclerosis (glomerular hyperfunction alone does little to induce glomerular hypertrophy and sclerosis). The physical loss of nephrons, in addition to the loss of their excretory function, is required to trigger glomerular hypertrophy and sclerosis [10].

The causes and consequences of the dysregulation of NO in hypertension and other renal disease processes continue to be important topics for investigation [11]. The present study aims to analyse the renal cortical structural remodelling when chronically L-NAME-induced hypertensive rats are simultaneously treated, or not, with angiotensin converting enzyme (ACE) inhibitor or calcium channel blocker (CCB).

## Material and methods

### Sample and procedures

Thirty-two mature male rats (Wistar strain) were obtained from colonies maintained at the State University of Rio de Janeiro. In the beginning of the study the animals had a body mass of 266.1±21.1g and a systolic blood pressure (SBP) of 116.0±5.1mmHg (mean±SD). All animals were individually housed in a temperature (21±1°C) and humidity-controlled (60±10%) room submitted to a 12h-dark/light cycle (artificial lights, 7:00–19:00h) and air exhaustion cycle (15min/h). Rats received food (Nuvilab®, Rio de Janeiro, Brazil) and water *ad libitum*. The university standing committee on animal research had approved the protocols. The investigation conforms to the “Guide for

the Care and Use of Laboratory Animals” published by the US National Institutes of Health (NIH Publication No.85-23, revised 1996).

Animals stayed the first week for acclimatization. During this period, the minimum water intake *per animal* was determined as 50ml/day. This volume was used to dissolve drugs and guarantee the total intake of the planned daily drug dosage.

The SBP and the body mass were weekly verified in all rats. The SBP was verified using the non-invasive method of the tail-cuff plethysmography (RTBP1007, Kent Scientific Co., Litchfield, USA). After the acclimatization period, animals were maintained alive for six weeks. Four groups of eight rats each were treated according to the following outline: **Control group (C)**: animals were manipulated and sacrificed just as the animals of the experimental groups; they only received water and food *ad libitum*. **L-NAME group (L)**: animals received L-NAME 50mg/kg/day dissolved in drinking water (hydrochloride of N $\omega$ -nitro-L-arginine-methyl-ester) (Sigma Chemical Co., St. Louis, Lot 67H0876). **L-NAME+Enalapril group (L+E)**: animals received L-NAME (dose and administration way indicated for Group L-NAME) and, simultaneously, enalapril maleate 15mg/kg/day dissolved in drinking water ((S)-N-(1-(Ethoxycarbonyl)-3-phenylpropyl)-Ala-Pro maleate) (Sigma Chemical Co., St. Louis, Lot 38H0500). **L-NAME+Verapamil group (L+V)**: animals received L-NAME (dose and administration way indicated for Group L-NAME) and, simultaneously, verapamil hydrochloride 15mg/kg/day dissolved in drinking water (Sigma Chemical Co., St. Louis, Lot 56H0925).

### Tissue processing

In the morning of the 43rd day of experimentation animals were deeply anaesthetised and sacrificed (heart injection of 3ml of KCl at 10%). The kidneys were excised by shortly cutting the renal pedicle, and the kidney volume (KV) was determined according to the submersion method of Scherle [12], in which the water displacement due to KV is recorded by weighting (KW). As the specific gravity (g) of isotonic saline is 1.0048 the KV is obtained by:  $KV = KW/g$ , or simple  $KV \approx KW$  [13].

The cortical/medullar (CM) ratio was estimated by Cavalieri’s method in one left kidney of each group, the areas of cortical and the medullar profiles were measured by point counting under microscopic view using a regular square grid [14]. This was important to estimate the absolute stereological parameters, as described below.

The renal cortex of the left kidneys was analysed by stereology, according to the vertical section design. The kidneys were divided in two halves and both were placed

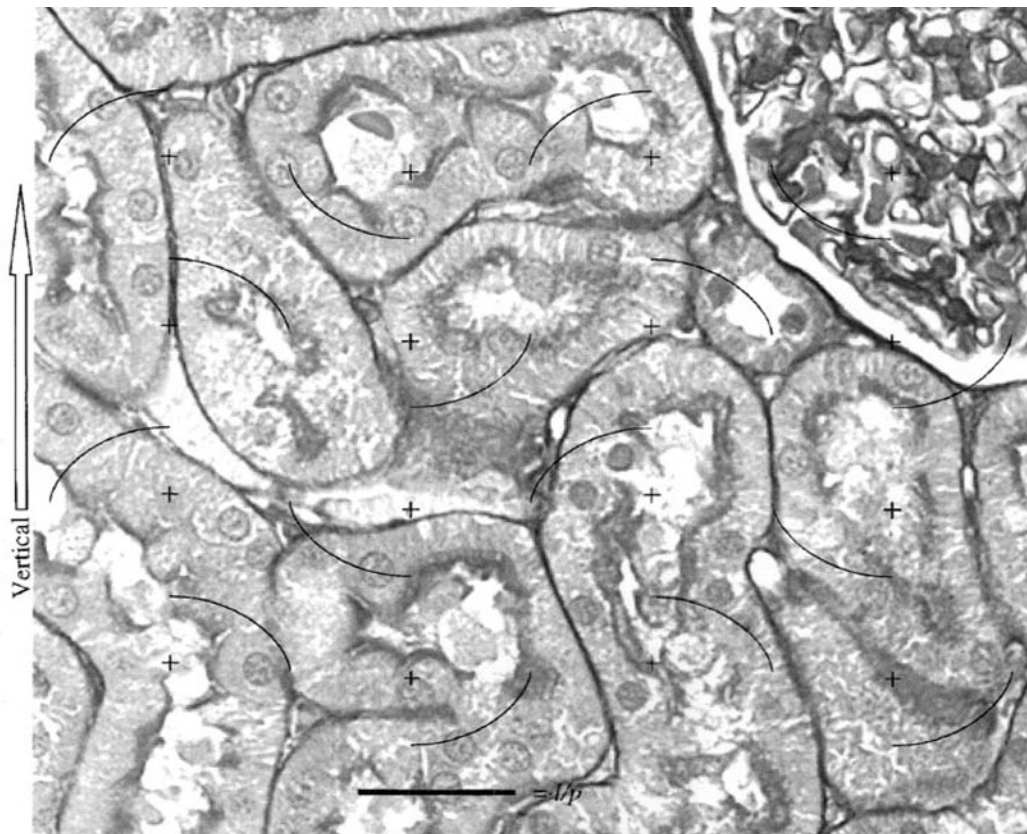


**Fig. 1** Counts in the left renal cortex used a test-system with cycloids where the minor axes of the cycloids were arranged in parallel with the defined vertical axis (bar=25 $\mu$ m).

on the cut surface. One half was randomly rotated and the other half was 90° rotated with respect to the first. Both halves were placed 48h at room temperature in fixative (freshly prepared 4% w/v formaldehyde in 0.1M phosphate buffer pH 7.2), embedded in Paraplast plus® and four vertical sections were systematic uniformly random sampled [15]. Sections had 3 $\mu$ m of thickness and were stained with hematoxylin-eosin or Masson's trichrome.

### Stereology and statistical analysis

Four microscopic fields by animal were analysed using a video-microscope (Leica model DMRBE microscope, Kappa CF 15/5 video-camera and a Sony triniton monitor), a test-system with cycloids was put upon the screen of the monitor and calibrated (Leitz micrometer 1mm/100). The minor axes of the cycloids were arranged in parallel with the defined vertical axis that is demonstrated in the Fig. 1. The number of intersections between the surface traces and the cycloid arcs ( $I_L$ ) was

counted to estimate the glomerulus (glomerular tuft and capsule) and the cortical tubules surface densities ( $S_v = 2 \cdot I_L$ ). The reference volume was estimated by point counting using the test points that hit the renal cortex ( $P_T$ ). The number of points hitting the glomerulus, tubules and vessels ( $P_p$ ) was counted to estimate the volume densities of these structures ( $V_v = P_p / P_T$ ). The number of the tubules was counted in a two-dimensional test frame area ( $Q_A$ ) of 6,400 $\mu$ m<sup>2</sup> allowing estimate of the tubule length density ( $L_v = 2 \cdot Q_A$ ). By multiplying these densities by the cortical volume determined through the Scherle method and the CM ratio, the total estimates surface (S), volume (V) and length (L) were derived.

The estimate of the volume-weighted mean glomerular volume (VWGV) was made through the "point-sampled intercepts" method [16]. For this procedure five fields were analysed per section, three sections of the kidney, eight animals per group (120 fields per group). A test-system consisting of parallel

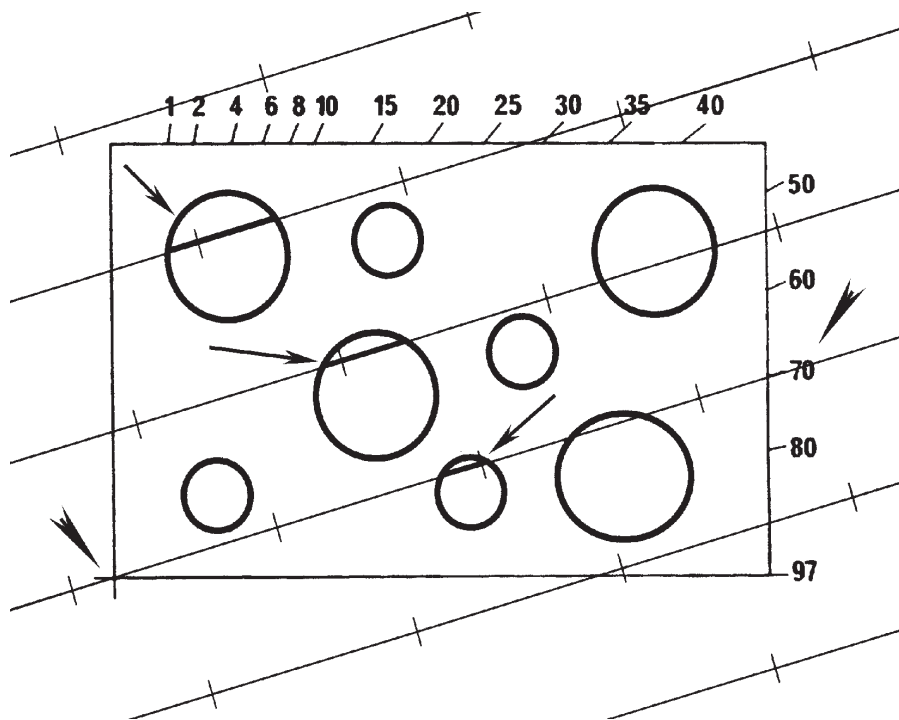


**Fig. 2** Schematic representation of the test-system consisting of parallel lines associated with test points used to determine the glomeruli to be measured. The direction of the lines on the sample was determined by lottery and aligned with the edge indications of the frame (arrow heads). The line length was measured for each glomerulus selected by the test-point inside the unbiased counting frame (arrows). The  $l_0^3$ -ruler is showed in the bottom of the figure.

lines associated with test points was superposed on each microscopic field. The direction of the lines on the sample was determined by lottery. For each point inside the unbiased counting frame, which hits a glomerulus intercept through the point was measured that is demonstrated in the Fig. 2. The measurement of the intercept length was performed using a 32-mm long logarithmic  $l_0^3$ -ruler composed of a series of 15 classes, where the width of any class is, approximately, 17% larger than the preceding class [17]. Each individual intercept was cubed, and the mean of all values was multiplied by  $\pi/3$  in every case to obtain VWGV.

The differences of the SBP and the biometrical parameters among the groups were tested by the analysis of variance and the multiple comparison Newman-Keuls test. The SBP weekly difference into a group was tested with the paired t-test. The stereological differences among the groups were tested using the non-parametric Kruskal-Wallis analysis of variance and, in cases where differences were found, the Kolmogorov-Smirnov test was used. In all cases the significant level of 0.05 was considered for significant statistics [18].

## Results

### The systolic blood pressure

The analysis of the SBP variation demonstrated that the enalapril and the verapamil administration was efficient to reduce the SBP in the respective rats submitted to NOs blockade (Fig. 3). The L group, SBP grew significantly since the 2<sup>nd</sup> week until the 6<sup>th</sup> week (when the L group SBP was, approximately, 80% higher than the C group); each subsequent week had a significant SBP increase. In the L+E and L+V groups the SBP only grew in the 2<sup>nd</sup> and 3<sup>rd</sup> weeks, reaching the C group levels after this period until the end of the experimentation.

### The renal cortex structure and stereology

The microscopic appearance of the cortical structures was normal in the C group and showed minimal lesions in the L+E and L+V groups.

**Table 1** Effects of L-NAME, L-NAME+Enalapril, L-NAME+Verapamil assessed by left renal cortex stereology. The volume of the right and left kidneys (RKV and LKV, respectively), tubular volume, tubular length, volume-weighted mean glomerular volume were evaluated under different drug regimens. The groups are: C: control, L: L-NAME, L+E: L-NAME+Enalapril, L+V: L-NAME+Verapamil. L[tubule]: tubular length, V[tubule]: tubular volume, VWGV: volume-weighted mean glomerular volume.

Groups	RKV (mm <sup>3</sup> )	LKV (mm <sup>3</sup> )	V[tubule] (mm <sup>3</sup> )	L[tubule] (mm (x10 <sup>4</sup> ))	VWGV (mm <sup>3</sup> )
C	776±46	785±53	327±42	89±7	0.6±0.2
L	934±80	906±79	508±67	62±9	1.2±4.0
L+E	812±44	797±42	358±60	81±7	0.8±0.3
L+V	785±49	776±52	386±54	79±10	0.8±0.2
	ANOVA		Kruskal-Wallis		
	0.008	0.03	0.0009	0.0002	0.004
	Newman-Keuls test		Kolmogorov-Smirnov test		
C vs. L	S	S	S	S	S
C vs. L+E	NS	NS	NS	NS	NS
C vs. L+V	NS	NS	NS	NS	NS
L vs. L+E	S	S	S	S	S
L vs. L+V	S	S	S	S	S
L+E vs. L+V	NS	NS	NS	NS	NS

However, all glomeruli had important alterations in L group rats, characterized by glomerular hypertrophy and also global or segmental glomerular sclerosis. The renal parenchyma had some glomeruli presenting an atrophic structure as well as tubular atrophy and extensive fibrosis, and

hypertrophied glomeruli frequently had capsular thickening.

The BM had no variation among the groups. Even the right and left kidneys had a volume 20% greater in L group rats than the C group rats, while both sides KV was significantly smaller in L+E and

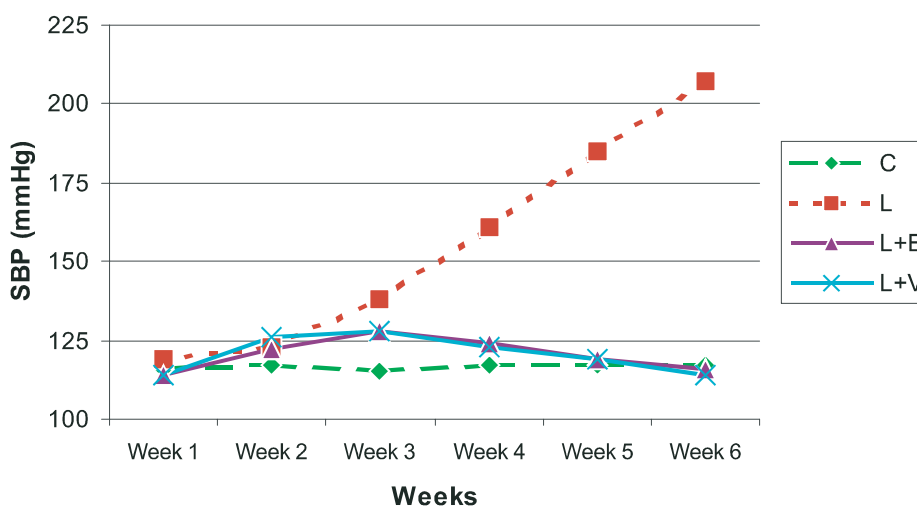


**Fig. 3** Effects of L-NAME, L-NAME+Enalapril, L-NAME+Verapamil upon systolic blood pressure (SBP). The groups are: C: control, L: L-NAME, L+E: L-NAME+Enalapril, L+V: L-NAME+Verapamil.



L+V groups than in L group, but no difference was found among L+E, L+V and C animals. The VWGV had the same variation seen in the KV, but with a greater magnitude. The VWGV was 100% greater in L group rats than the C group rats, while the VWGV was significantly smaller in L+E and L+V groups than in L group (30% smaller).

Considering the absolute parameters the V[tubule] was 30-50% greater, while the L[tubule] was 20-30% smaller in the L group than in the other groups (Table 1).

## **Discussion**

The normotensive rats with chronic NOs blockade develop hypertension and consequently the renal cortex structure is altered. The main renal cortical changes due to NOs blockade seen in the present work was as the glomerular sclerosis (due to the hypertensive classic lesion of the glomerulus) as the glomerular hypertrophy (determined by the increased VWGV), and the tubular remodelling characterized by dilatation and shortness (determined by the increased V[tubule] and the decreased L[tubule], respectively). These results confirm previous reports in the literature concerning normotensive rats and NOs blockade [2, 7, 11, 19-20].

Other hypothesis investigated by the present study was the reversibility of the cortical lesions in animals treated with ACE inhibitor or CCB. The present study design did not allow us to know if installed lesions due to NOs blockade could be completely reverted to a normal cortical structure, but it demonstrated that both enalapril and verapamil were efficient to prevent the glomerular sclerosis or hypertrophy, as well as the tubular remodelling when administered together with the L-NAME, probably because they significantly reduce the blood pressure. Nevertheless, this subject is still controversial: the antisclerotic potency of the antihypertensive therapy appears to be related to the drugs potency to inhibit glomerular growth rather than an effect on the abnormal hemodynamics developed in the glomerulus [21-22]. On the other hand, treatment with ACE inhibitor reduces blood pressure, proteinuria, and glomerulosclerosis, but equihypotensive treatment

with a CCB does not reduce proteinuria and delay but did not prevent glomerulosclerosis. Thus, in the rat similar reductions in SBP with these two classes of agents have disparate effects on the progression of chronic renal failure [23]. The CCB nitrendipine failed to sustain the beneficial effect on kidney morphology and urinary albumin excretion in long-term diabetes and hypertensive rats SHR [24]. However, chronic CCB verapamil administration was shown to reduce the renal dysfunction, glomerular sclerosis, and mortality in partially nephrectomized rats, but the mechanism is still unknown [25].

The apoptosis, or the programmed cell death, is a mechanism of tissue remodelling that occurs in hypertensive rats submitted to NOs blockade [26-27] and could explain some of the present findings. Apoptosis contributes to tissue remodelling and recovery of normal tissue structure, but cell turnover in the healthy glomerulus is low [28]. However, in the presence of acute inflammation the rate of apoptosis is consonantly increased. A 25- to 250-fold increase in glomerular apoptotic cells have been described in human poststreptococcal glomerulonephritis and experimental Thy-1 nephritis [29-30]. When a high apoptotic rate of renal parenchymal cell persists beyond the recovery of normal tissue cellularity, it leads to the loss of renal parenchymal cells that characterizes glomerular sclerosis or tubular atrophy [31]. Evidence from experimental models of renal injury suggests that apoptosis coexists with renal cell proliferation; these cells may be more sensitive to absolute or relative deficits in survival factors [32-33], such as hypertension/hypoxia mechanism [34] and NO/superoxide [35-36]. There are no doubts that apoptosis not only plays a key role in renal physiology, but could also be a potential pathogenetic mechanism, when inappropriate, in maintaining inflammation in injured kidneys or in inducing progressive scarring [37].

The renin-angiotensin system plays a prominent role in the development of hypertension in the NOs blockade model [38]. The angiotensin II has been clearly demonstrated to induce both cellular proliferation [39-40] and apoptosis [41-42]. Recent study demonstrated that the angiotensin type 2 receptor is expressed in the adult rat kidney and promotes cellular proliferation and apoptosis in the

proximal tubular epithelial cells [43]. This could explain the beneficial effect of the ACE inhibitor enalapril on the cortex region of the rat kidney with NOs blockade other than the simple control of the blood pressure. This beneficial effect of the ACE inhibitor is also demonstrated on the myocardial necrosis/fibrosis despite the presence of arterial hypertension [44-45]. The assumption that the angiotensin type 2 (AT2) receptor is decisive for a beneficial effect of the ACE inhibitor in these experiments should be supported by further studies using a specific AT2 inhibitor.

The present study of the renal cortical region observed glomerular sclerosis/hypertrophy and tubular remodelling in hypertensive rats with NOs blockade, which was efficiently prevented by the simultaneous treatment with enalapril or verapamil.

## Acknowledgements

The authors would like to thank CNPq and Faperj Brazilian agencies for their financial support to this research.

## References

1. **Moncada S., Palmer R.M.J., Higgs E.A.**, Nitric oxide: physiology, pathophysiology, and pharmacology. *Pharmacol. Rev.*, **43**: 109-142, 1991
2. **Just A.**, Nitric oxide and renal autoregulation, *Kidney Blood Press. Res.*, **20**: 201-204, 1997
3. **Baylis C., Mitruka B., Deng A.**, Chronic blockade of nitric oxide synthesis in the rat produces systemic hypertension and glomerular damage, *J. Clin. Invest.*, **90**: 278-281, 1992
4. **Fujihara C.K., Michellazzo S.M., DeNucci G., Zatz R.**, Sodium excess aggravates hypertension and renal parenchymal injury in rats with chronic NO inhibition, *Am. J. Physiol.*, **266 (Renal Fluid Electrolyte Physiol 35)**: F697-F705, 1994
5. **Majid D.S.A., Navar L.G.**, Nitric oxide in the mediation of pressure natriuresis, *Clin. Exp. Pharmacol. Physiol.*, **24**: 595-599, 1997
6. **Stoos B.A., Garvin J.L.**, Actions of nitric oxide on renal epithelial transport, *Clin. Exp. Pharmacol. Physiol.*, **24**: 591-594, 1997
7. **Liang M., Knox F.G.**, Production and functional roles of nitric oxide in the proximal tubule, *Am. J. Physiol.*, **278 (Regulatory Integrative Comp Physiol)**: R1117-R1124, 2000
8. **Qiu C., Muchant D., Neierwaltes W.H., Racusen L., Baylis C.**, Evolution of chronic nitric oxide inhibition hypertension, *Hypertension*, **31**: 21-26, 1998
9. **Ikenaga H., Ishii N., Didion S.P., Zhang K., Cornish K.G., Patel K.P., Mayhan W.G., Carmines P.K.**, Suppressed impact of nitric oxide on renal arteriolar function in rats with chronic heart failure, *Am. J. Physiol.*, **276 (Renal Physiol. 45)**: F79-F87, 1999
10. **Yoshida Y., Fogo A., Ichikawa I.**, Glomerular hemodynamic changes vs. hypertrophy in experimental glomerular sclerosis, *Kidney Int.*, **35**: 654-660, 1989
11. **Schnackenberg C., Patel A.R., Kirchner K.A., Granger J.P.**, Nitric oxide, the kidney and hypertension, *Clin. Exp. Pharmacol. Physiol.*, **24**: 600-606, 1997
12. **Scherle W.**, Simple method for volumetry of organs in quantitative stereology, *Mikroskopie*, **26**: 57-60, 1970
13. **Weibel E.W.**, Stereological methods. Practical methods for biological morphometry, Academic Press, London, 1979
14. **Gundersen H.J.G., Bendtsen T.F., Korbo L., Marcussen N., Møller A., Nielsen K., Nyengaard J.R., Pakkenberg B., Sørensen F.B., Vesterby A., West M.J.**, Some new, simple and efficient stereological methods and their use in pathological research and diagnosis, *A.P.M.I.S.*, **96**: 379-394, 1988
15. **Nyengaard J.R.**, Stereological methods and their application in kidney research, *J. Am. Soc. Nephrol.*, **10**: 1100-1123, 1999
16. **Gundersen H.J.G., Jensen E.B.**, Stereological estimation of the volume weighted mean volume of arbitrary particles observed on random sections, *J. Microsc.*, **138**: 127-142, 1985
17. **Sørensen F.B.**, Stereological estimation of the mean and variance of nuclear volume from vertical sections, *J. Microsc.*, **162**: 203-229, 1991
18. **Zar J.H.**, Biostatistical analysis, Prentice-Hall, Upper Saddle River, 1999
19. **Raij L.**, Nitric oxide in hypertension: relationship with renal injury and left ventricular hypertrophy, *Hypertension*, **31[part 2]**: 189-193, 1998
20. **Pereira L.M.M., Mandarim-de-Lacerda C.A.**, Glomerular profile numerical density per area and mean glomerular volume in rats submitted to nitric oxide synthase blockade, *Histol. Histopathol.*, **16**: 15-20, 2001
21. **Bauer J.H.**, Modern antihypertensive treatment and the progression of renal disease, *J. Hypertens.*, **16(Suppl. 5)**: S17-S24, 1998
22. **Yoshida Y., Kawamura T., Ikoma M., Fogo A., Ichikawa I.**, Effects of antihypertensive drugs on glomerular morphology, *Kidney Int.*, **36**: 626-635, 1989

23. **Tolins J.P., Raij L.**, Comparison of converting enzyme inhibitor and calcium channel blocker in hypertensive glomerular injury, *Hypertension*, **16**: 452-461, 1990
24. **Nielsen B., Grønbaek H., Osterby R., Flyvbjerg A.**, Effect of the calcium channel blocker nitrendipine in normotensive and spontaneously hypertensive, diabetic rats on kidney morphology and urinary albumin excretion, *J. Hypertens.*, **17**: 973-981, 1999
25. **Pelayo J.C., Harris D.C.H., Shanley P.F., Miller G.J., Schrier R.W.**, Glomerular hemodynamic adaptations in remnant nephrons: effects of verapamil, *Am. J. Physiol.*, **254 (Renal Fluid Electrolyte Physiol 23)**: F425-F431, 1998
26. **Mandarim-de-Lacerda C.A., Pereira L.M.M.**, Numerical density of cardiomyocytes in chronic nitric oxide synthesis inhibition, *Pathobiol.*, **68**: 36-42, 2000
27. **Gomes-Pessanha M., Mandarim-de-Lacerda C.A.**, Influence of the chronic nitric oxide synthesis inhibition on cardiomyocytes number, *Virchows Arch.*, **437**: 667-674, 2000
28. **Savill J.S., Mooney A.F., Hughes H.**, Apoptosis in acute renal inflammation. In: Neilson E.G., Couser W.G., eds., Immunologic renal disease, Lippincott-Raven, Philadelphia, 1998, pp. 209-219
29. **Shimizu A., Kitamura H., Masuda Y., Ishizaki M., Sugisaki Y., Yanamaka N.**, Apoptosis in the repair process of experimental proliferative glomerulonephritis, *Kidney Int.*, **47**: 114-121, 1995
30. **Shimizu A., Masuda Y., Kitamura H., Ishizaki M., Sugisaki Y., Yamanaka N.**, Recovery of damaged glomerular capillary network with endothelial cell apoptosis in experimental proliferative glomerulonephritis, *Nephron*, **79**: 206-214, 1998
31. **Sugiyama H., Kashiwara N., Makino H., Yamasaki Y., Ota A.**, Apoptosis in glomerular sclerosis, *Kidney Int.*, **49**: 103-111, 1996
32. **Thomas G.L., Yang B., Wagner B.E., Savill J., El Nahas A.M.**, Cellular apoptosis and proliferation in experimental renal fibrosis, *Nephrol. Dial. Transplant.*, **13**: 2216-2226, 1998
33. **Davis M.A., Ryan D.H.**, Apoptosis in the kidney, *Toxicol. Pathol.*, **26**: 810-825, 1998
34. **Saikumar P., Dong Z., Patel K., Hall K., Hopfer U., Weinberg J.M., Venkatachalam M.A.**, Role of hypoxia-induced Bax translocation and cytochrome c release in reoxygenation injury, *Oncogene*, **17**: 3401-3415, 1998
35. **Sandau K., Pfeilschifter J., Brune B.**, Nitric oxide and superoxide induced p53 and Bax accumulation during mesangial cell apoptosis, *Kidney Int.*, **52**: 378-386, 1997
36. **Aiello S., Remuzzi G., Noris M.**, Nitric oxide/endothelin balance after nephron reduction, *Kidney Int.*, **53 (Suppl. 65)**: S63-S67, 1998
37. **Amore A., Coppo R.**, Role of apoptosis in pathogenesis and progression of renal diseases, *Nephron*, **86**: 99-104, 2000
38. **Ribeiro M.O., Antunes E., DeNucci G., Lovisolo S.M., Zatz R.**, Chronic inhibition of nitric oxide synthesis. A new model of arterial hypertension, *Hypertension*, **20**: 298-303, 1992
39. **Bunkenburg B., Van Amelsvoort T., Rogg H., Wood J.M.**, Receptor mediated effects of angiotensin II on growth of vascular smooth muscle cells from spontaneously hypertensive rats, *Hypertension*, **20**: 746-754, 1992
40. **Kunert R.J., Stepien H., Komorowski J., Pawlikowski M.**, Stimulatory affect of angiotensin II on the proliferation of mouse spleen lymphocytes *in vitro* is mediated via both types of angiotensin II receptors, *Biochem. Biophys. Res. Commun.*, **198**: 1034-1039, 1994
41. **Tanaka M., Ohnishi J., Ozawa Y., Sugimoto M., Usuki S., Naruse M., Murakami K., Miyazaki H.**, Characterization of angiotensin II receptor type 2 during differentiation and apoptosis of rat ovarian cultured granulosa cells, *Biochem. Biophys. Res. Commun.*, **207**: 593-598, 1995
42. **Kajstura J., Cigola E., Malhotra A., Li P., Cheng W., Meggs L.G., Anversa P.**, Angiotensin II induces apoptosis of adult ventricular myocytes *in vitro*, *J. Mol. Cell. Cardiol.*, **29**: 859-870, 1997
43. **Cao Z., Kelly D.J., Cox A., Casley D., Forbes J.M., Martinello P., Dean R., Gilbert R.E., Cooper M.E.**, Angiotensin type 2 receptor is expressed in the adult rat kidney and promotes cellular proliferation and apoptosis, *Kidney Int.*, **58**: 2437-2451, 2000
44. **Matsubara B.B., Matsubara L.S., Franco M., Padovani J.C., Janicki J.S.**, The effect of non-antihypertensive doses of angiotensin converting enzyme inhibitor on myocardial necrosis and hypertrophy in young rats with renovascular hypertension, *Int. J. Exp. Pathol.*, **80**: 97-104, 1999
45. **Mandarim-de-Lacerda C.A., Pereira L.M.M.**, Volume-weighted mean nuclear volume and numerical density in the cardiomyocyte following enalapril and verapamil treatment, *Virchows Arch.*, **438**: 92-95, 2001